19th International Conference on the Application of Computer
Science and Mathematics in Architecture and Civil Engineering
K. Gürlebeck, T. Lahmer and F. Werner (eds.)
Weimar, Germany, 04–06 July 2012

INFLUENCE OF DIFFERENT DATA TYPES FOR THE ESTIMATION OF HYDROMECHANICAL PARAMETERS FOR A WATER RETAINING DAM USING SYNTHETIC DATA

José G. De Aguinaga

Research Training Group 1462, Bauhaus-Universität Weimar
Berkaer Str. 9, 99423 Weimar, Germany
E-mail: jose.de.aguinaga@uni-weimar.de

Keywords: Sensitivity analysis, Parameter identification, Particle Swarm Optimization, Embankment.

Abstract. *The present research analyses the error on prediction obtained under different data availability scenarios to determine which measurements contribute to an improvement of model prognosis and which not.*

A fully coupled 2D hydromechanical model of a water retaining dam is taken as an example. Here, the mean effective stress in the porous skeleton is reduced due to an increase in pore water pressure under drawdown conditions.

Relevant model parameters are ranked by scaled sensitivities, Particle Swarm Optimization is applied to determine the optimal parameter values and model validation is performed to determine the magnitude of error forecast. We compare the predictions of the optimized models with results from a forward run of the reference model to obtain actual prediction errors.

The analyses presented here were performed to 31 data sets of 100 observations of varying data types. Calibrating with multiple information types instead of only one sort, brings better calibration results and improvement in model prognosis. However, when using several types of information the number of observations have to be increased to be able to cover a representative part of the model domain; otherwise a compromise between data availability and domain coverage prove best.

Which type of information for calibration contributes to the best prognoses, could not be determined in advance. For the error in model prognosis does not depends on the error in calibration, but on the parameter error, which unfortunately can not be determined in reality since we do not know its real value. Excellent calibration fits with parameters' values near the limits of reasonable physical values, provided the highest prognosis errors. While models which included excess pore pressure values for calibration provided the best prognosis, independent of the calibration fit.

1 INTRODUCTION

There has been a growing need to better understand model quality of numerical models in all branches of science. This issue has been recently addressed by [1, 2, 3, 4, 5] among others.

Models have grown in complexity and scope. In civil engineering, different models have to be coupled to simulate behavior of complex structures. Type, location and quality of measurements significantly impact model calibration and validation in these coupled models. This information either contributes to model quality by improving model forecast or to model uncertainty when neglecting important information. Models have to be parameterized; however, the values of the parameters are usually not known and have to be calibrated by inverse methods using observations [6]. This study focus on the influence of using different observation types for calibration on model prediction.

An advantage of calibrating with different observation types is to overcome systematic errors. Systematic errors are difficult to detect and cannot be analyzed statistically, because all of the data is off in the same direction, either too high or too low. The approach to overcome this is similar to that of investing in stokes of different branches, the risk of having the wrong numbers is disperse. Experience with the specific data type and measurement conditions are required to detect this errors. A way around this is to use different types of observations for calibration. If one set is wrong the others will push the values still in the right direction. By working with many data sets, even if you do not notice that one of them is wrong, the model could still be calibrated properly by the weight of other ”correct” data sets.

To analyze the effects of the observation types in the numerical model, the drawdown of an embankment will serve as illustrative example. This is a typical flow and deformation coupled problem in geotechnical engineering.

It is not the goal of this paper to find the best model description for hydromechanical models, but to quantify the error related to model calibration with different data type availability. The objective is to identify the data relationships which are necessary to correctly predict deformation, strain and excess pore pressure development within a coupled hydromechanical model.

2 METHODOLOGY

A reference model of a water retaining dam is generated to assess the impact of data availability to model error prognosis. Such a model provides different types of synthetic measurements, in this case, under slow drawdown conditions. The same model can be then, calibrated to all possible combinations of these measurement sets. Finally, the models with the optimized sets of parameters can be validated under rapid drawdown conditions and the prognosis error be compared.

With the reference model we create a total of five different data sets: horizontal and vertical deformation, horizontal and vertical strain and excess pore pressure. Based on these sets we generate 31 combinations ($2^{5\ \text{data types}}$ - 1 = 31 data sets) of equal number of observations but different type of data. In order to determine the effect of ”data type” in model forecast, we calibrate the more important parameters to the different 31 data sets using the same model which generated the data. This is necessary to avoid external influences other than data type, and compare their forecasts to the reference model.

Before calibration, a sensitivity analysis is performed to determine the most important parameters of the model. The optimal parameter values are identified with Particle Swarm Op-

timization on a surrogate model. Finally, the calibrated models are validated under a rapid drawdown scenario and the actual forecast errors are determined.

3 THEORY

Single scaled sensitivities ($ss_{i,j}$) are used to determine the most relevant parameters of the model. They provide the ratio of difference in model response at each *i* measuring point (y_i) to a small change in parameter value of every *j* parameter (p_j) where *i,j* $\in \mathbb{N}$. They are calculated as follow [7]:

$$ss_{i,j} = \frac{\partial y_i}{\partial p_j} p_j \tag{1}$$

In matrix form the scaled sensitivity matrix (SS) can be calculated as

$$\mathrm{SS} = \frac{\partial \mathrm{y}}{\partial \mathrm{p}} \mathrm{p} \tag{2}$$

where y is the calculated model response vector $\{y_1, y_2, ..., y_i\}$ and p is the model parameter vector $\{p_1, p_2, ..., p_j\}$. The partial derivatives are approximated by forward finite difference:

$$\frac{\partial \mathrm{y}}{\partial \mathrm{p}} \approx \frac{\mathrm{y(p} + \Delta \mathrm{p)} - \mathrm{y(p)}}{\Delta \mathrm{p}} \tag{3}$$

The resulting sensitivities are ranked calculating the variance-covariance matrix, $(\mathrm{SS^T SS})^{-1}$, which is the inverted product of the transposed scaled sensitivity matrix times itself. The smaller the value of the respective parameter in the main diagonal of the variance covariance matrix, the more influential the parameter is.

The divergence between model response and reference measured values is quantified by the objective function as follows:

$$F(\mathrm{p}) = \sqrt{\sum_{i=1}^{n} \frac{(y_{i,meas} - y_i(p_1, p_2, ..., p_n)_{calc})^2}{\sum_{j=1}^{n} y_{i,meas}^2} w_i} \tag{4}$$

where $F(\mathrm{p})$ is the average error sum, $i = 1, 2, ..., n$ counts each measurement of a time series, and w is a weighting factor, in this case equal to one. In $F(\mathrm{p})$ the absolute error of all observation types is sumed and then squared to get an average. The objective funtion sums unitless values. This is achieved for each type of data by norming the squared residuals of a given type at each measuring point, by the squared sum of the measurements at the given point.

An automated calibration is performed with Particle Swarm Optimization [8] using the following surrogate model:

$$y(\mathrm{p})_{calc} = \hat{y}(\mathrm{p}, \beta) + \hat{\epsilon} \tag{5}$$

by this means the numerical model is approximated with a fully quadratic function, $\hat{y}(\mathrm{p}, \beta)$, for each time step [9]. Where β are the coefficients of the fully quadratic approximation and $\hat{\epsilon}$ is the error between numerical and surrogate model.

During optimization the sum of the objective function for each measurement series is minimized:

$$F_{total}(\mathrm{p}) = \frac{1}{m}\sum_{j=1}^{m} F_j(\mathrm{p}) \rightarrow min. \tag{6}$$

where m stands for the amount of test series.

4 ILLUSTRATIVE EXAMPLE: WATER RETAINING DAM

A numerical model of a water retaining dam under drawdown conditions is used to illustrate the data availability influence on error prognosis of coupled numerical models in constructive civil engineering. The simulations were performed with PLAXIS 2D [10], a commercial Finite Element Program.

4.1 Geometry and boundary conditions

The earth dam is of trapezoidal form (Figure 1), 30 m high, trapezoid upper side is only 5 m long while the bottom side is 172.5 m long, from which 20 m correspond to the core. The underline block is 260 m long and also 30 m height. The extension of this block was conceived large enough to avoid effects of the boundary conditions inside the dam.

The mesh was constructed with 6-node triangular elements refined on the embankment itself and consists of around 500 elements and ca. 1100 nodes. On Figure 1 it is also marked the initial water level at 25 m (straight line) and the final water level at 5 m (dashed line).

Furthermore, the boundary condition at the bottom of the rectangular block is of full fixity, no deformation in horizontal or vertical direction allowed. At the sides just vertical deformation is allowed while the entire upper boundary is a free surface with a time dependent water level.

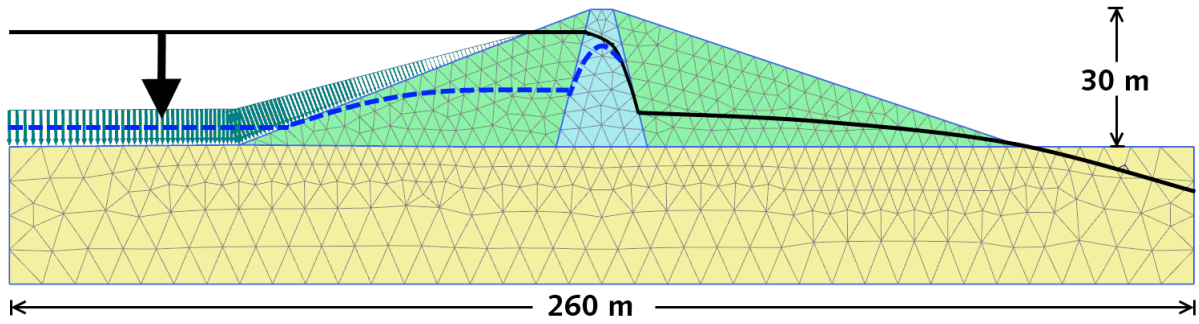

Figure 1: Mesh of water retaining dam with core (trapezoid in the center), fill (lateral triangles) and subsoil (rectangular basement), showing schematic drawdown and water pressure distribution

4.2 Material model

The embankment has three distinctive parts of different materials which have to be parameterized: 1) an almost impermeable clay core to prevent flow through it; 2) the fill, normally constructed of local material to protect the core from erosion and forces applied by the water; and 3) the subsoil which is the foundation in which the dam is built on.

For all three soil materials, the Mohr-Coloumb model (MC) is used to represent the elastic-plastic soil behavior. MC is suitable to analyze the stability of slopes and embankments [11].

The hydraulic model is parameterized using the Hypres data set available in PLAXIS with Van Genuchten parameterization. This parameterization is of coarse subsoil type for fill and subsoil material and of very fine type for the core.

The values of the parameters are given in Table 1 and are synthetic since they were not determined from an existing object.

Table 1: Soil parameter values for the three different materials

Soil parameters		Core	Fill	Subsoil
		Undrained	Drained	Drained
Saturated soil unit weight	γ_{unsat} [kN/m^3]	16	16	17
Unsaturated soil unit weight	γ_{sat} [kN/m^3]	18	20	21
Shear Modulus	G [kN/m^2]	555.60	7518.80	19230.77
Poisson's ratio	ν' [-]	0.35	0.33	0.30
Cohesion	C'_{ref} [kN/m^2]	5	5	1
Friction angle	φ' [°]	25	31	35
Dilatancy angle	ψ [°]	0	1	5
Hydraulic conductivity (isotropic)	k_{xy} [m/d]	0.0001	0.25	0.01

4.3 Simulation

The hydraulics in PLAXIS are simulated with the Darcy law for fully saturated soil and with the Richards equation which describes unsaturated groundwater flow. They are fully coupled to the mechanical model using Biot's theory of consolidation. This formulation contains a coupled hydromechanical behaviour represented by both the equilibrium equation and the continuity equation of the water-soil mixture [12].

Calculations are performed in classical mode, which uses Terzaghi's definition of stress. In a first phase, the initial stress due to soil and material weight is calculated, as well as the initial pore water pressure under undrained behaviour and steady state groundwater flow conditions.

To the previous Gravity loading phase follows a Nil-Step phase. This phase improves the accuracy of the equilibrium stress field with a plastic drained long term calculation in which no additional loading is applied [13]. Finally, the effect of the drawdown can be simulated as a consolidation phase with transient groundwater flow in which the dam is submitted to a linear drawdown of 40 cm/d.

5 RESULTS AND CONCLUSIONS

5.1 Sensitivities

The Parameters of interest for the present study are those of the soft soil core, specially the isotropic hydraulic conductivity (k_{xy}), two parameters from Hooke's law: shear modulus (G) and Poisson's ratio (ν') and also the parameter to describe the flow rule, the dilatancy angle (ψ). Since we are working on the range of values where the dam is stable and cannot sample data about its collapse, the parameters to define failure are not of interest for this study, these are the friction angle and cohesion.

Eight nodes and five stress points within the core and the fill (Figure 2) were selected for

measurements of five different types of data: horizontal and vertical deformation (u_x, u_y), horizontal and vertical strain ($\varepsilon_{xx}, \varepsilon_{yy}$) and excess pore pressure (*EPP*)

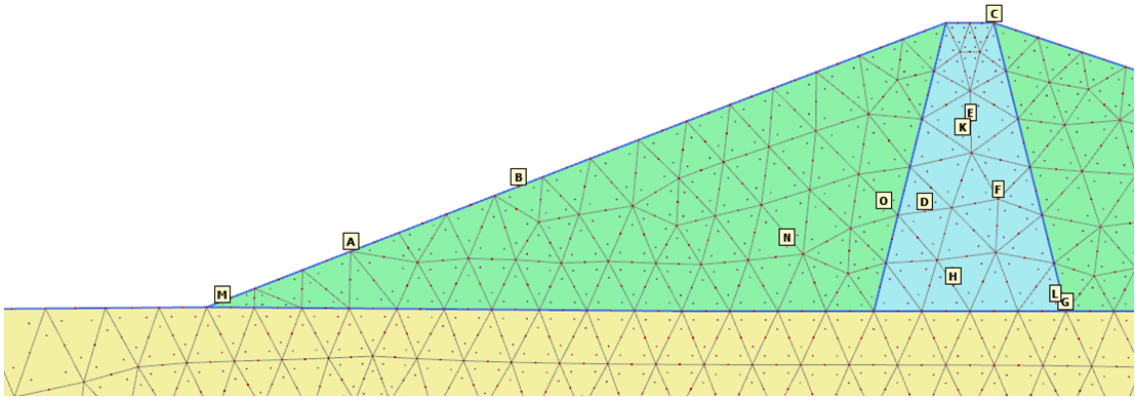

Figure 2: Observation points at the embankment

The Sensitivities were calculated with respect to the five different types of model answers at those observation points using the equations presented on Section 3. The resulting variance-covariance matrix is shown on Table 2. The smaller the value on the diagonal, the more sensitive the respective parameter is.

Table 2: Variance-Covariance Matrix $(SS^TSS)^{-1}$ of the most relevant parameters of the impermeable core

		G	ν'	ψ	$\lg(k_{xy})$	
G	[	$\mathbf{4 \cdot 10^{-4}}$	$-8 \cdot 10^{-5}$	$2 \cdot 10^{-3}$	$-3 \cdot 10^{-6}$	]
ν'	[		$\mathbf{7 \cdot 10^{-5}}$	$7 \cdot 10^{-5}$	$-1 \cdot 10^{-7}$	]
ψ	[			$\mathbf{1 \cdot 10^{-1}}$	$-1 \cdot 10^{-6}$	]
$\lg(k_{xy})$	[		symmetric		$\mathbf{6 \cdot 10^{-7}}$	]

The more influential parameter is k_{xy} from the hydraulic model followed by G and ν' from Hooke's law of the material model.

5.2 Calibration

The four previous parameters, which were sensitive to a set of model answers of diverse type in 13 different points, were calibrated to different data type availability. 31 data sets, shown in Table 3, each with 100 observations were generated from the combinations of $u_x, u_y, \varepsilon_{xx}, \varepsilon_{yy}$ and *EPP*.

The resulting combinations have a constant number of observations and vary in data type. This generates a tradeoff between data type coverage and spatial domain coverage. The spatial coverage of the first data set, considering all data types is shown at the left side of Figure 3. Measured in nodes A and B are u_x and u_y, *EPP* in nodes B and C, and $\varepsilon_{xx}, \varepsilon_{yy}$ in the stress points K and L. In contrast, at the right side of Figure 3, data set 31, which uses just *EPP* observations, shows a good spatial coverage of *EPP* in the core. As data type increases, spatial coverage decreases and vice versa.

The model was calibrated to the 31 data sets with an automated algorithm using the Particle Swarm Optimization method on a surrogate model. The resulting deviations to the respective data sets are also given on Table 3 as average error sum in percent.

Table 3: Combinations of data type availability for calibration purpose using 100 observations; number of points per data type (10 measurements in time per point) and resulting average error sum [%]

	1	2	3	4	5	6	7	8	9	10	11	12	13	14	15	16
u_x	2	3	2	2	3		3	3	3	4	3	3				
u_y	2	2	2	2		3	3	3	3				4	3	3	
ε_{xx}	2	3	3		2	2	4			3	3		3	3		3
ε_{yy}	2	2		3	2	2		4		3		3	3		3	3
EPP	2		3	3	3	3			4		4	4		4	4	4
Error	0.8	0.2	0.6	0.9	0.9	1.0	0.1	0.1	0.9	0.3	0.9	0.3	0.0	1.1	0.7	1.4

	17	18	19	20	21	22	23	24	25	26	27	28	29	30	31
u_x	5	5	5	5							10				
u_y	5				5	5	5					10			
ε_{xx}		5			5			5	5				10		
ε_{yy}			5			5		5		5				10	
EPP				5			5		5	5					10
Error	0.2	0.0	0.2	0.1	0.1	0.6	0.7	0.2	1.1	1.7	0.1	0.2	0.9	0.7	1.5

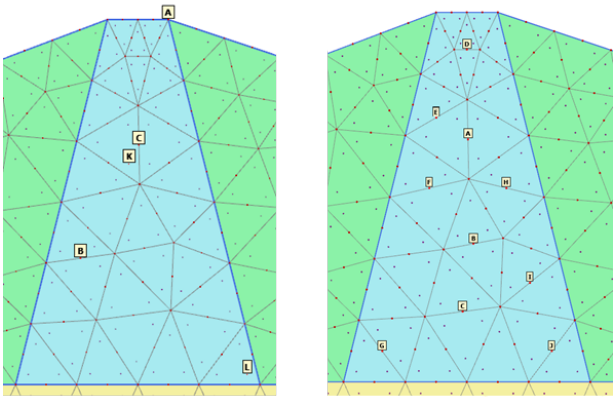

Figure 3: Left: Observation points for data set 1, ; Right: Observation points for data set 31

The average error sum for all different calibrations is small, lower than 2 %. After sorting the average error three classes were identified, as shown in Figure 4. These are, a first class with excellent fit, up to 0.3 % average error (green oval), a second class with good fits on the range 0.5 - 1.2 % average error (orange oval) and a third class with relative bad fits from 1.4 to 1.7 % average error (red oval). Most of the calibrations fall within the first two classes.

Furthermore, by sorting Figure 4 additionally by number of data types, see Figure 5, we can determine that the best results are obtained by using 1 to 3 data types, however, also the worst values. The choice of data type makes then the difference between best or worst case. It must be noticed that most of the best calibration results can be attained with 2 and 3 data types. This reflects the tradeoff between using different data types for calibration vs. the spatial coverage of each single data type. For our case with 100 observations, a set with two or three data types, might allow for variety in information for calibration while maintaining some representative spatial coverage of the domain.

Every data type is used 16 times in different combinations. The calibrations using combinations of data sets with u_x show the best fits, see Figure 6. In contrast, the worst fits are obtained

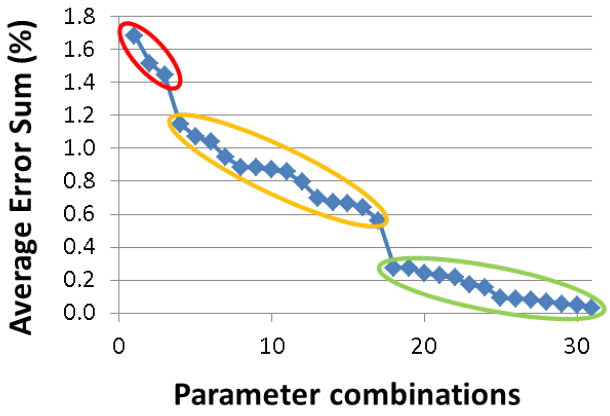

Figure 4: Sorted average error sum of calibration results for different parameter combinations

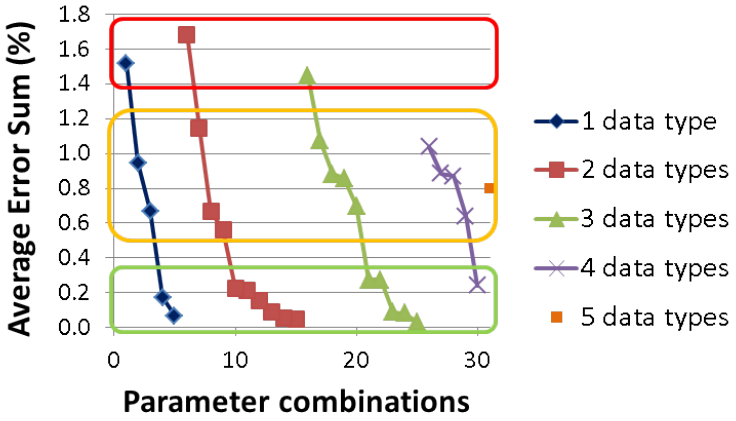

Figure 5: Sorted average error sum of calibration results by number of data types used

when *EPP* is considered.

5.3 Validation

The model was validated for each of the resulting optimal parameter values. For this, 90 observations were taken on the 5 days period in which the water table decreased at a linear rate of 4 m per day.

The average error sums of the validations were lower than those obtained during calibration. However, the average error sums of both graphs are not comparable in magnitude, since the validation values were measured at different points, at different times, with fewer measurements and what is more important with other boundary conditions (under rapid falling water table). What can be compared are the tendencies to analyze if there are correlations between them.

The maximum prediction average error sum was around 1 %, see Figure 7. Most of the validation results fall within the range 0.3 and 0.7 % average error sum.

When the average error sum of the prognosis is sorted also by number of data types, see Figure 8 we see a similar trend as with the calibration results. The best and worst fits are obtained with 2 or 3 types of data.

Which parameters are responsible for the best and worst cases is appreciable in Figure 9,

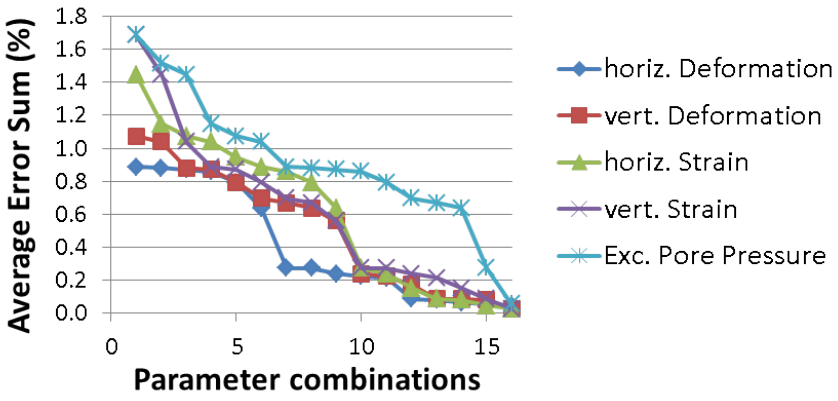

Figure 6: Sorted average error sum of calibration results by data type

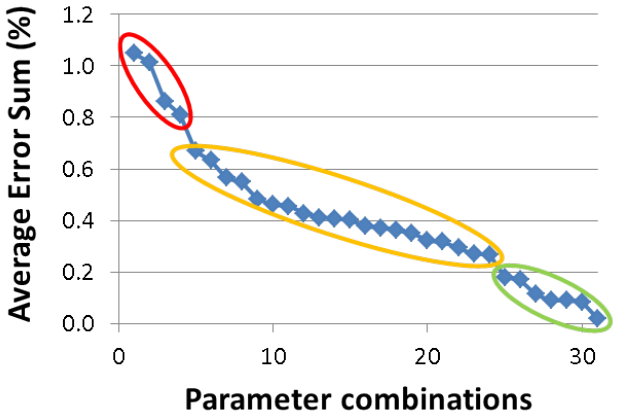

Figure 7: Sorted average error sum of validation results for different parameter combinations

where the results are sorted by type of observation used for calibration. Surprisingly the worst prognosis were made by considering deformation or strain observations during calibration. In contrast, a guarantee for good prognosis seemed to be attained by calibrating with *EPP* information. This is the opposite as deducted from Figure 6, in which calibrating with deformation while excluding *EPP* information is recommended to obtain best calibration results.

By plotting the sorted calibration results against the actual errors of the prognosis (left side of Figure 10), we observe that a decrease in calibration error does not improve the prognosis accuracy. The prognosis error seems to be normal distributed around 0.4 % average error sum. However, for the case of excellent calibration fits with average error sums lower than 0.3 % the validation error becomes more variable, and the parameter set is susceptible of giving prognosis with higher errors.

The right side of Figure 10 shows the corresponding parameter error of the optimized parameter sets at the left side of the Figure. By very small calibration errors, the optimized parameter values can be driven to values close to the limit of reasonable physical values, as it was here the case for several combinations for k_{xy}, which is the most sensitive parameter in this model.

5.4 Conclusion

The fit obtained by the automated Particle Swarm Optimization calibration was very good, with an average error sum at all cases lower than 2 %. However, the error in prognosis does not

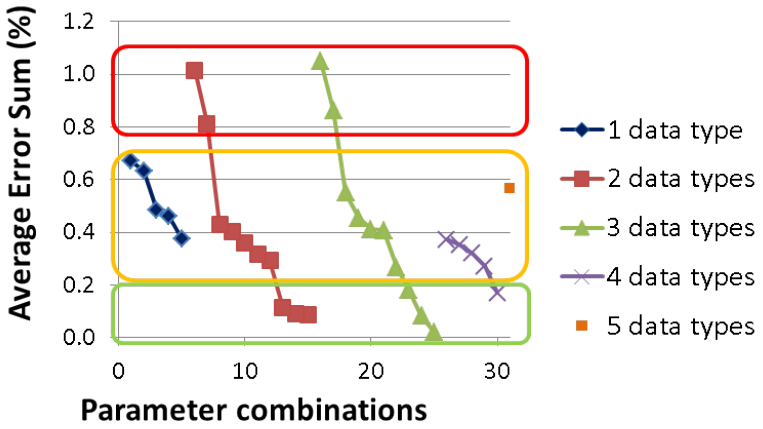

Figure 8: Sorted average error sum of validation results by number of data types used

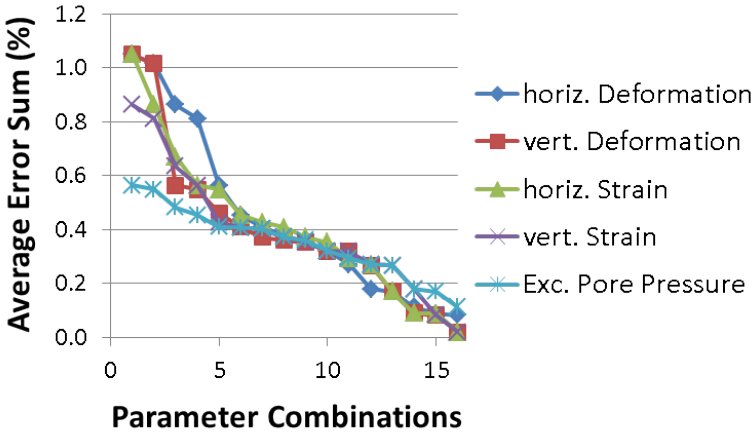

Figure 9: Sorted average error sum of validation results by data type

correlate with the calibration effort, since when calibration error decreases, validation error does not. Excellent calibration values, interestingly increased the variation in prognosis error. These calibrations, with very small errors can drive the value of the optimized parameters to the limit of reasonable physical values, as it is here the case. The error of the prognosis depends on the parameter error. Unfortunately, the parameter error can not be determined since we normally do not know the real value of the parameter.

Surprisingly, the model calibrated to all five different types did not provide the best results. This could be explained by the reduction of the spatial coverage. Using 2 or 3 types of information, both, best and worst calibrations were obtained. Depending on which data sets are considered, either the best or the worst results are obtained. The best calibrations usually were obtained considering u_x while the worst calibrations included a data set of *EPP*. The opposite was the case for the prognosis. Good prognosis were attained with the data sets which considered *EPP* for calibration, while the worst prognosis were given by those considering u_x for calibration. The information that contributes to the best prognoses, could not be determined in advance. Information diversity for calibration and a good coverage of model domain is important for a good prognosis. In order to obtain better prognosis it is preferable to accept higher calibration errors and obtain optimized parameter values which are more likely to be expected

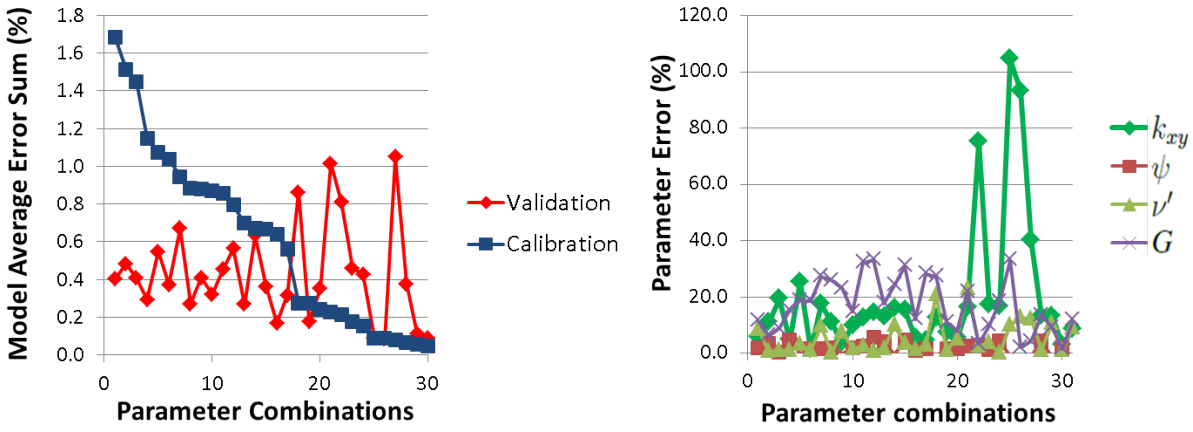

Figure 10: Left: sorted average error sum of calibration results with corresponding validation error. Right: Corresponding parameter errors

than excellent calibration fits with unreasonable parameter values. This could be implemented in an automated optimization algorithm by using the expected value of the parameters as prior information for calibration [14].

6 ACKNOWLEDGMENTS

The author would like to acknowledge the support of Dr. Martin Zimmerer for allowing the use of his optimization code VARO^{2}PT, which interacts with PLAXIS and the support by the German Research Council (DFG) through the Research Training Group 1462.

REFERENCES

[1] S. Nishat, Y. Guo and B. W. Baetz, Relative Importance of Input Parameters in the Modeling of Soil Moisture Dynamics of Small Urban Areas. *Journal of Hydrologic Engineering*. **17** (3), 2012. ISSN 1084-0699/2012/3-359-367.

[2] H. Keitel and A. Dimmig-Osburg, Uncertainty and sensitivity analysis of creep models for uncorrelated and correlated input parameters. *Engineering Structures*, 2010. doi:10.1016/j.engstruct.2010.08.020

[3] T. Most, Estimating uncertainties from inaccurate measurement data using maximum entropy. K. Gürlebeck and C. Könke eds. *18th International Conference on the Application of Computer Science and Mathematics in Architecture and Civil Engineering*, Weimar, Germany, 07-09 July 2009.

[4] L. J. Lucas, H. Owhadi and M. Ortiz, Rigorous verification, validation, uncertainty quantification and certification. *Comput. Methods Appl. Mech. Engrg.*, **197**, 4591–4609, 2008. doi:10.1016/j.cma.2008.06.008.

[5] I. Babuška, F. Nobile and R. Tempone, Reliability of Computational Science. *Numerical Methods for Partial Differential Equations*, **23** (4), 753–784, 2007. doi: 10.1002/num.20263.

[6] T. Lahmer, Crack identification in hydro-mechanical systems with applications to gravity water dams. *Journal of Inverse Problems in Science and Engineering*, **18** (8), 1083–1101, 2010. doi:10.1080/17415977.2010.500495.

[7] M. M. Zimmerer, Identifikation konstitutiver Parameter von weichen feinkörnigen Böden, Beitrag zum Konsolidationsverhalten von Ton. Dissertation, Bauhaus-Universität Weimar, *Schriftenreihe des DFG Graduiertenkollegs 1462 Modellqualitäten*, **1**, 2010.

[8] J. Kennedy, R. Eberhard, Particle Swarm Optimization. *Proc. IEEE International Conference on Neuronal Networks*, 1942–1948, Perth, Australia, 27 Nov. - 01 Dec. 1995.

[9] M. M. Zimmerer, T. Schanz, Y.Lins and V. Bettzieche, Numerical Analysis of Water Reservoir Dam - Prediction of Long Term Performance of Versetal Dam (Germany). *79th ICOLD Annual Meeting*, Lucerne, Switzerland, May 29 - June 3, 2011.

[10] R. B. J. Brinkgreve, W. M. Swolfs, E. Engin, D. Waterman, A. Chesaru, P. G. Bonnier and V. Galavi, PLAXIS 2D 2010 (Version 2010.01). Delft, Netherlands: PLAXIS b.v., 1997-2010. Available at http://www.plaxis.nl

[11] K. S. Ti, B. B. K. Huat, J.Noorzaei, M. S. Jaafar, and G. S. Sew, A Review of Basic Soil Constitutive Models for Geotechnical Application. *Electronic Journal of Geotechnical Engineering*, **14** (J), 1–18, 2010.

[12] V. Galavi, Groundwater flow, fully coupled flow deformation and undrained analyses in PLAXIS 2D and 3D. Internal Report, Delft, Netherlands: PLAXIS b.v. Research Department, January 2010. Available at: http://kb.plaxis.nl/author/v-galavi

[13] PLAXIS b.v., PLAXIS Scientific Manual 2010. Delft, Netherlands: PLAXIS b.v., 2010. Available at http://www.plaxis.nl/shop/135/info/manuals/

[14] A.J. Jakeman, R.A. Letcher and J.P. Norton, Ten iterative steps in development and evaluation of environmental models. *Environmental Modelling & Software*, **21** (5), 602–614, May 2006. doi: 10.1016/j.envsoft.2006.01.004